A&A 469, 553–560 (2007)
DOI: 10.1051/0004-6361:20066579


Astronomy & Astrophysics

# Self-consistent treatment of dynamics and chemistry in the winds from carbon-rich AGB stars

## I. Tests of the equilibrium and kinetic chemical codes⋆

M. Pułecka[1], M. R. Schmidt[1], V. I. Shematovich[2], and R. Szczerba[1]

[1] N. Copernicus Astronomical Center, Rabiańska 8, 87–100 Toruń, Poland
e-mail: mara@ncac.torun.pl
[2] Institute of Astronomy, Russian Academy of Sciences, Pyatnitskaya 48, Moscow, Russian Federation

Received 17 October 2006 / Accepted 27 February 2007

**ABSTRACT**

*Aims.* The main aim of this paper was to test our (chemical and kinetic) codes, which will be used during self-consistent modelling of dynamics and chemistry in the winds from C-rich AGB stars.
*Methods.* We used the thermodynamical equilibrium code to test the different databases of dissociation constants. We also calculated the equilibrium content of the gas using the kinetic code that includes the chemical network of neutral-neutral reactions. The influence of reaction rates updated using the UMIST database for Astrochemistry 2005 (UDFA05) was tested.
*Results.* The local thermodynamical equilibrium calculations show that the NIST database reproduces equilibrium concentrations fairly well in comparison with previous computations, while consistency for the other, commonly used, dissociation constants is worse.
The most important finding is that the steady state solution obtained with the kinetic code for the reactions network is different from the thermodynamical equilibrium solution. In particular, the important opacity sources CN and $C_2$ are underabundant relative to thermodynamical equilibrium, while O-bearing molecules (like SiO, $H_2O$, and OH) are overabundant. After updating the reaction rates by data from the UDFA05 database, the consistency in O-bearing species becomes much better, however the disagreement in C-bearing species is still present.

**Key words.** astrochemistry – stars: AGB and post-AGB – stars: carbon – stars: atmospheres – stars : circumstellar matter – stars: winds, outflows

## 1. Introduction

Asymptotic giant branch (AGB) stars develop a molecular dusty wind driven by radiation pressure on dust grains condensating in the warm molecular layers. The newly formed molecules and dust are then deposited into the interstellar medium (ISM) where they contribute to the global matter budget of galaxies. Therefore, the determination of molecular and dust contents in the AGB winds is important for understanding their further reprocessing in the ISM before matter eventually ends up in new star-forming regions.

The chemical evolution of gas around AGB stars takes place in different conditions. These include thermodynamical equilibrium in stellar photospheres, non-equilibrium (including possible shock-induced) chemistry, dust formation, and photon-dominated chemistry in circumstellar envelopes.

Observations of circumstellar envelopes in the infrared and millimetre range demonstrate that they are very rich in molecules. In the case of the well-studied, C-rich AGB star, IRC+10 216 the number of identified molecules exceeds 60 (Olofsson 2006). The majority of the observed molecules are carbon-chain molecules such as the cyanopolyynes, the hydrocarbon radicals and carbenes, as well as organo-sulphur and organo-silicon molecules. Interferometric and single-dish observations show that carbon-chain molecules are distributed in the hollow shells around a central star. This distribution has been interpreted as arising from the photochemistry of parent molecules (e.g. $C_2H_2$ and HCN) flowing away from the star (see e.g. reviews by Glassgold 1996; Millar 2003). The new space and ground-based projects (e.g. Stratospheric Observatory for Infrared Astronomy – SOFIA, The Atacama Large Milimeter Array – ALMA or Herschel Space Observatory) will allow us to investigate the circumstellar molecular inventory in much more detail by using the not yet fully exploited, sub-millimetre range.

With the aim of preparing tools for analysing the new sub-millimetre observations of AGB stars, we are in the process of developing a self-consistent treatment of the dynamics and chemistry in circumstellar envelopes. The first effort to build the chemical network of reactions for conditions close to thermodynamical equilibrium (high density and temperature) in a C-rich environment was made by Willacy & Cherchneff (1998, hereafter WC98). Since the considered densities are high and effective temperature of the star is low, only neutral-neutral bimolecular and termolecular reactions were considered. WC98 investigated the chemistry of sulphur and silicon in the inner wind of IRC+10216. Their non-equilibrium calculations started from chemical composition derived at the local thermodynamical equilibrium (LTE) conditions. It was found that the parent molecules $C_2H_2$ and CO are unaffected by the shocks, but the abundances of daughter molecules can be significantly

⋆ Figures 3–5 and 7 are only available in electronic form at http://www.aanda.org

altered by the shock-driven chemistry. Their model indicated that molecule production by the shock-driven chemistry close to the photosphere can be significantly greater than the LTE chemistry. Recently, Cherchneff (2006) has investigated the chemistry and composition of the quasi-static molecular layers of AGB stars using the same semi-analytical model of shock dynamics as in WC98.

In modelling stellar atmospheres it is commonly assumed that the conditions of local thermodynamical equilibrium prevails. Molecular content is then defined by dissociation constants. In the outflow where the shocks are present, kinetic equations must be solved for given chemical network. When local thermodynamical equilibrium is valid at some position in the stellar atmosphere, both approaches should produce the same molecular concentrations. If not, then an inconsistency will appear, obscuring the interpretation of the results. The aim of our paper is to clarify this point for future application of available chemical networks for non-equilibrium computations of the chemistry in the inner layers of carbon-rich outflows.

In this paper we present our steady-state chemical code and test (some of) the available chemical databases against work of WC98. In the next paper (Schmidt et al. in preparation), we will discuss our approach to self-consistent treatment of dynamics and chemistry. The first preliminary results of these computations were presented by Pulecka et al. (2005a, with the TITAN hydrodynamical code) and Pulecka et al. (2005b, using the FLASH hydrodynamical code).

## 2. Test of chemical codes: the thermodynamical equilibrium

In stellar photospheres the dynamical timescales are much longer than the timescales of molecular formation (Glassgold 1996). Therefore, to determine local molecular contents it is sufficient to apply the thermodynamical equilibrium (TE) conditions. To compute molecular composition in the local TE conditions, one needs to know the temperature ($T$), the total gas number density ($n$), or equivalently the total gas pressure ($p$), and the initial elemental abundances. We have constructed such a TE code and present the results of our tests.

### 2.1. The thermodynamical equilibrium code

The equilibrium chemistry code is based on the Russell (1934) approach. This method uses the fictitious pressure $p_{\rm f}$(X), which is the pressure exerted by element X if all the gas were in the neutral form of the atomic species X. The fictitious pressure of element X is thus given by

$$p_{\rm f}({\rm X}) = p_{\rm X} + \sum_{\rm Y} \alpha_{\rm X,Y} p_{\rm Y}, \quad (1)$$

where $p_{\rm Y}$ is the partial pressure[1] of molecular species Y, which contains element X, $\alpha_{\rm X,Y}$ is the stoichiometric coefficient indicating the number of element X involved in molecule Y. For example, in the case of hydrogen we have

$$p_{\rm f}({\rm H}) = p_{\rm H} + 2p_{\rm H_2} + p_{\rm CH} + 2p_{\rm CH_2} + ... \quad (2)$$

(plus all examined hydrogen-bearing molecules).

The partial pressure of compound X is related to its concentration $n_{\rm X}$ [cm$^{-3}$] by the ideal gas law $p_{\rm X} = n_{\rm X}\,k\,T$ [dyn cm$^{-2}$], where $k$ is the Boltzmann constant [erg/K], and $T$ is the temperature [K]. Using the partial pressures, the dissociation constant ($K_{\rm p}$) of molecule AB (AB → A + B) can be expressed as

$$K_{\rm p}({\rm AB}) = \frac{p_{\rm A} p_{\rm B}}{p_{\rm AB}} = \frac{n_{\rm A}\,kT\,n_{\rm B}\,kT}{n_{\rm AB}\,kT} = \frac{n_{\rm A}\,n_{\rm B}}{n_{\rm AB}}\,kT, \quad (3)$$

where $p_{\rm A}$, $p_{\rm B}$, $p_{\rm AB}$ are the partial pressures of atoms A, B, and molecule AB, and $n_{\rm A}$, $n_{\rm B}$, $n_{\rm AB}$ are the their concentrations. Therefore by employing Eq. (3), the fictitious pressure of hydrogen can be rewritten to

$$p_{\rm f}({\rm H}) = p_{\rm H} + 2\frac{p_{\rm H}^2}{K_{\rm p}({\rm H_2})} + \frac{p_{\rm H} p_{\rm C}}{K_{\rm p}({\rm CH})} + 2\frac{p_{\rm H}^2 p_{\rm C}}{K_{\rm p}({\rm CH_2})} + \cdots \quad (4)$$

Note that dissociation constants can be determined from the differences in the corresponding Gibbs free energies[2]. Since the fictitious pressure reflects the conservation of mass for element X, then $p_{\rm f}$(X) for any other atomic species X can be expressed in terms of the fictitious pressure of hydrogen $p_{\rm f}$(H):

$$p_{\rm f}({\rm X}) = A({\rm X}) p_{\rm f}({\rm H}), \quad (6)$$

where $A({\rm X}) = \frac{n_{\rm X}}{n_{\rm H}}$ is abundance of element X relative to hydrogen.

To close this set of nonlinear equations for fictitious pressures, we only need the equation for the total gas pressure, which is obtained by summing the partial pressures of all examined species. This final set of equations is solved using the Newton-Raphson method. The solution gives the partial pressure of atoms, which are then used to calculate the partial pressures of molecules (i.e. in fact their concentrations) by employing Eq. (3).

### 2.2. The equilibrium case of WC98

In a first test of our thermodynamical equilibrium code, we aimed to reproduce the thermodynamical equilibrium concentrations of species given in Table 3 of WC98. This table contains equilibrium abundances determined at a distance of $1.2\,R_*$ and physical conditions specified in the 1st entry of their Table 2 ($T = 2062$ [K] and $n = 3.68 \times 10^{14}$ [cm$^{-3}$], which corresponds to $p = 1.05 \times 10^2$ [dyn cm$^{-2}$]). To reproduce the equilibrium molecular content in these conditions, we need to know the initial elemental abundances and the dissociation constants.

The initial elemental abundances were determined by summing the abundances of all species (see Table 3 of WC98) containing a given element. The obtained values are given in Col. 2 of Table 1, where the abundance of element X is given by $\epsilon({\rm X}) = \log \frac{n_{\rm X}}{n_{\rm H}} + 12$, and $n_{\rm X}$ is the concentration of element X. For comparison, the solar abundances of H, He, C, O, N, Si, and S from Grevesse & Sauval (1998, hereafter GS98) and Asplund et al. (2005, hereafter A05) are shown in Cols. 3 and 4, respectively. The initial element abundances assumed by WC98 are essentially solar ones except for the C/O ratio, which was assumed to be about 1.5.

[1] The partial pressure of species Y is the pressure of the gas if no other species is presented in the medium.

[2] The change in ($\Delta G^\circ$) of products (A, B) and reactant (AB) is related to dissociation constant according to

$$K_{\rm p}(AB) = C^{\Delta\nu} \exp\left(-\frac{\Delta G^\circ}{RT}\right), \quad (5)$$

where $R = 8.32441 \times 10^7$ [erg K$^{-1}$ mol$^{-1}$] is the ideal gas constant, $C = 1.01325 \times 10^6$ [dyn cm$^{-2}$], and $\Delta\nu$ is the stoichiometric factor of a given dissociation reaction. The sign $^\circ$ marks conditions when the temperature is 273.15 K and the absolute pressure is 1 atm (i.e. 1.01325 bar, $1.01325 \times 10^6$ [dyn cm$^{-2}$], 101.325 [kPa]).

**Table 1.** The initial abundances of elements: $\epsilon(\mathrm{X}) = \log \frac{n_\mathrm{X}}{n_\mathrm{H}} + 12$.

| Element | WC98 | GS98 | A05 |
|---|---|---|---|
| (1) | (2) | (3) | (4) |
| H | 12.00 | 12.00 | 12.00 |
| He | 10.99 | 10.93 | 10.93 |
| C | 8.98 | 8.56 | 8.39 |
| N | 8.06 | 8.05 | 7.78 |
| O | 8.79 | 8.93 | 8.66 |
| Si | 7.49 | 7.55 | 7.51 |
| S | 7.19 | 7.33 | 7.14 |

The dissociation constants were obtained using species concentrations given in Table 3 of WC98 by employing Eq. (3). Note that the dissociation constants derived in such a way are valid *only* for the conditions (temperature) specified above. As expected, with these $K_\mathrm{p}$ and initial elemental abundances given in Col. 1 of Table 1, the obtained equilibrium concentrations are in very good agreement with values given in Table 3 of WC98. However, after discussion with K. Willacy, we realized that there are some misprints for the concentrations of $C_2$ and $SiH_4$ in Table 3 of WC98. Therefore, during further computation we implemented the original $\Delta G^\circ$'s (kindly provided by Willacy) from the work of WC98. These $\Delta G^\circ$'s are now collected in Table 2 (Cols. 3 and 8), and used to determine the equilibrium species concentrations that will be referred to hereafter as WC98 concentrations. The molecules listed in this table (with ordinal numbers in Cols. 1 and 6) are organised in order of decreasing WC98 concentrations.

### 2.3. Comparison of TE concentrations based on WC98, NIST, and Tsuji databases

As described in Sect. 2.2, determination of TE concentrations at specified conditions requires knowledge of $K_\mathrm{p}$ (or equivalently $\Delta G^\circ$). The most comprehensive database, which is publicly available and allows computation of dissociation constants, is that collected by the National Institute of Standards and Technology (NIST). The NIST chemistry WebBook[3] provides thermochemical data, such as the enthalpy of formation ($H^\circ$) and molar entropy ($S^\circ$) for different temperatures at standard conditions. These quantities allow determination of the Gibbs free energy ($G^\circ$) for all examined species according to

$$G^\circ = H^\circ - T\,S^\circ. \tag{7}$$

Thus, we can determine the difference in Gibbs free energies ($\Delta G^\circ$) for products and reactants, of the direct dissociation of molecule into single atoms, and use them to find the dissociation constants from Eq. (5).

We computed concentrations of species according to the method described in Sect. 2.1, using the dissociation constants obtained from the NIST database for $T = 2062$ [K]. The NIST database does not contain thermochemical data for some molecules: $C_3H$ – #9 (number appearing after symbol # is the ordinal number of a given molecule used in Fig. 1), $C_4H_2$ – #16, HCS – #25, $C_4H$ – #26, HCSi – #27, HNSi – #28, $SiH_2$ – #29, $SiCH_2$ – #30, $C_3H_2$ – #31, $SiH_3$ – #37, so we have used $\Delta G^\circ$'s from WC98, instead. The comparison between NIST and WC98 concentrations is shown in Fig. 1. The order of species (except for elements on the right side of the figure) follows decreasing concentrations of WC98. The consistency is fairly good (almost all results agree within about 7%, with the exception of the $SiC_2$ – #11 concentration, for which the difference is about 22%.

From a chemical point of view, a better illustration of discrepancies between different databases of thermochemical data is a comparison between $\Delta G^\circ$'s. Therefore, in Cols. 4 and 9 of Table 2 we provide the $\Delta G^\circ$ values derived from the NIST database. We left empty spaces for species with missing data in that database. In Fig. 2 we plotted the differences between $\Delta G^\circ$ from NIST and WC98 (circles) for each species. Again, the order of species (except for elements on the right side of the figure) follows decreasing concentrations of WC98. For molecules without data in the NIST database, there are no corresponding symbols in Fig. 2. As one can see, energies agree within about 2 [kJ mol$^{-1}$] with the exception of $SiC_2$ for which the discrepancy is about 5 [kJ mol$^{-1}$].

Another widely used database, especially in the modelling of stellar atmospheres, is the set of dissociation constants compiled by Tsuji (1973). The thermal dependence of $K_\mathrm{p}$ in this database is given by

$$\log K_\mathrm{p} = c_0 + c_1\theta + c_2\theta^2 + c_3\theta^3 + c_4\theta^4, \tag{8}$$

where $c_{i,i=0,1,\ldots,4}$ are coefficients derived by Tsuji and $\theta = \frac{5040}{T}$. This equation allows us to compute dissociation constants at the temperature of interest ($T = 2062$ K). The corresponding $\Delta G^\circ$, computed from Eq. (5), are collected in Cols. 5 and 10 of Table 2, and compared with WC98 values and NIST values in Fig. 2. The Tsuji database does not contain seven molecules among the 46 considered: $C_4H_2$ – #16, HCS – # 25, $C_4H$ – #26, HCSi – #27, HNSi – #28, $SiCH_2$ – #30, and $C_3H_2$ – #31 (empty spaces in Table 2, and in Fig. 2). In general, agreement between $\Delta G^\circ$ from Tsuji and WC98 is worse than in the case of NIST. The largest differences are seen for CS – #7, CN – #10, $SiC_2$ – #11, SiH – #12, $C_3$ – #13, $CH_3$ – #15, $CH_2$ – #17, SiN – #23, $NH_2$ – #35, HCO – #36, and NS – #39. The $\Delta G^\circ$ values for other molecules differ less than about 4 [kJ/mol].

The influence of differences between the Tsuji and NIST $\Delta G^\circ$'s on species concentration can be seen in Fig. 3[4]. The order of species is same as in Fig. 1. We plotted there the logarithm of Tsuji concentrations relative to those of NIST (using the WC98 values of $\Delta G^\circ$ in the case of molecules with missing data). The consistency is rather poor. Concentrations for all molecules with considerable discrepancies in $\Delta G^\circ$ are significantly different, but additionally some other species reached a different equilibrium state. For example, for all sulfur-bearing species, except CS – #7 (i.e. SiS – #8, HS – #14, $H_2S$ – #21, HCS – #25, $S_2$ – #38, NS – #39, SO – #45, S – #53), we see very large discrepancies (even by a factor of 84! for $S_2$), in spite of the fact that differences between $\Delta G^\circ$'s are significant only in the cases of CS and NS. Among other molecules with significant discrepancies in concentrations are those containing C: $C_3$ – #13, $CH_2$ – #17 and HCO – #36; two silicon-bearing molecules: SiN – #23 and SiH – #12; and radical $NH_2$ – #35.

### 2.4. The influence of changes in $\Delta G^\circ$ on the TE concentrations

In the first test of the influence of changes in $\Delta G^\circ$ on the equilibrium molecular content of examined gas, we only replaced the Tsuji $\Delta G^\circ$ for CS (this molecule has the highest equilibrium concentration among S-bearing molecules) by the lower value from the NIST database. The correlation between the Tsuji

[3] http://webbook.nist.gov/chemistry/

[4] Figures 3–5 and 7 are available only in the online version.

**Table 2.** $\Delta G^\circ$ in [kJ/mol] for $T = 2062$ K and $p = 1$ atm in case of WC98, NIST, and Tsuji (1973).

| # | Species | WC98 | NIST | TSUJI | # | Species | WC98 | NIST | TSUJI |
|---|---|---|---|---|---|---|---|---|---|
| (1) | (2) | (3) | (4) | (5) | (6) | (7) | (8) | (9) | (10) |
| 1 | $H_2$ | 207.6 | 206.1 | 205.6 | 24 | SiC | 215.4 | 214.5 | 213.9 |
| 2 | CO | 801.6 | 801.6 | 800.6 | 25 | HCS | 463.0 | | |
| 3 | $C_2H_2$ | 878.4 | 878.0 | 874.4 | 26 | $C_4H$ | 1279.8 | | |
| 4 | $N_2$ | 684.3 | 684.4 | 685.1 | 27 | HCSi | 386.0 | | |
| 5 | $C_2H$ | 676.0 | 675.8 | 673.0 | 28 | HNSi | 476.7 | | |
| 6 | HCN | 770.0 | 769.8 | 773.5 | 29 | $SiH_2$ | 150.4 | | 150.4 |
| 7 | CS | 453.8 | 453.2 | 501.1 | 30 | $SiCH_2$ | 555.8 | | |
| 8 | SiS | 372.7 | 371.4 | 370.8 | 31 | $C_3H_2$ | 1038.2 | | |
| 9 | $C_3H$ | 1049.7 | | 1050.0 | 32 | NH | 109.9 | 109.9 | 109.3 |
| 10 | CN | 507.0 | 507.1 | 519.1 | 33 | $H_2O$ | 455.4 | 455.4 | 455.4 |
| 11 | $SiC_2$ | 740.9 | 736.2 | 733.6 | 34 | $NH_3$ | 464.7 | 464.6 | 464.7 |
| 12 | SiH | 94.8 | 94.0 | 103.0 | 35 | $NH_2$ | 277.1 | 277.2 | 300.6 |
| 13 | $C_3$ | 794.3 | 793.5 | 851.1 | 36 | HCO | 662.7 | 662.5 | 716.0 |
| 14 | HS | 152.5 | 152.0 | 151.1 | 37 | $SiH_3$ | 280.9 | | 281.0 |
| 15 | $CH_3$ | 516.5 | 516.2 | 524.9 | 38 | $S_2$ | 183.7 | 183.4 | 186.9 |
| 16 | $C_4H_2$ | 1550.3 | | | 39 | NS | 262.4 | 261.7 | 282.0 |
| 17 | $CH_2$ | 318.8 | 318.6 | 282.5 | 40 | OH | 212.1 | 212.1 | 212.6 |
| 18 | CH | 131.7 | 131.6 | 129.1 | 41 | $H_2CO$ | 763.3 | 763.4 | 762.3 |
| 19 | SiO | 537.6 | 536.9 | 538.0 | 42 | $CO_2$ | 1024.3 | 1024.1 | 1023.1 |
| 20 | $C_2$ | 346.4 | 346.2 | 343.9 | 43 | $SiH_4$ | 335.1 | 333.9 | 336.9 |
| 21 | $H_2S$ | 286.8 | 286.2 | 288.4 | 44 | NO | 395.5 | 395.3 | 395.7 |
| 22 | $CH_4$ | 667.7 | 667.4 | 666.6 | 45 | SO | 279.3 | 278.7 | 279.2 |
| 23 | SiN | 317.3 | 316.6 | 261.4 | 46 | $O_2$ | 234.8 | 234.8 | 235.0 |

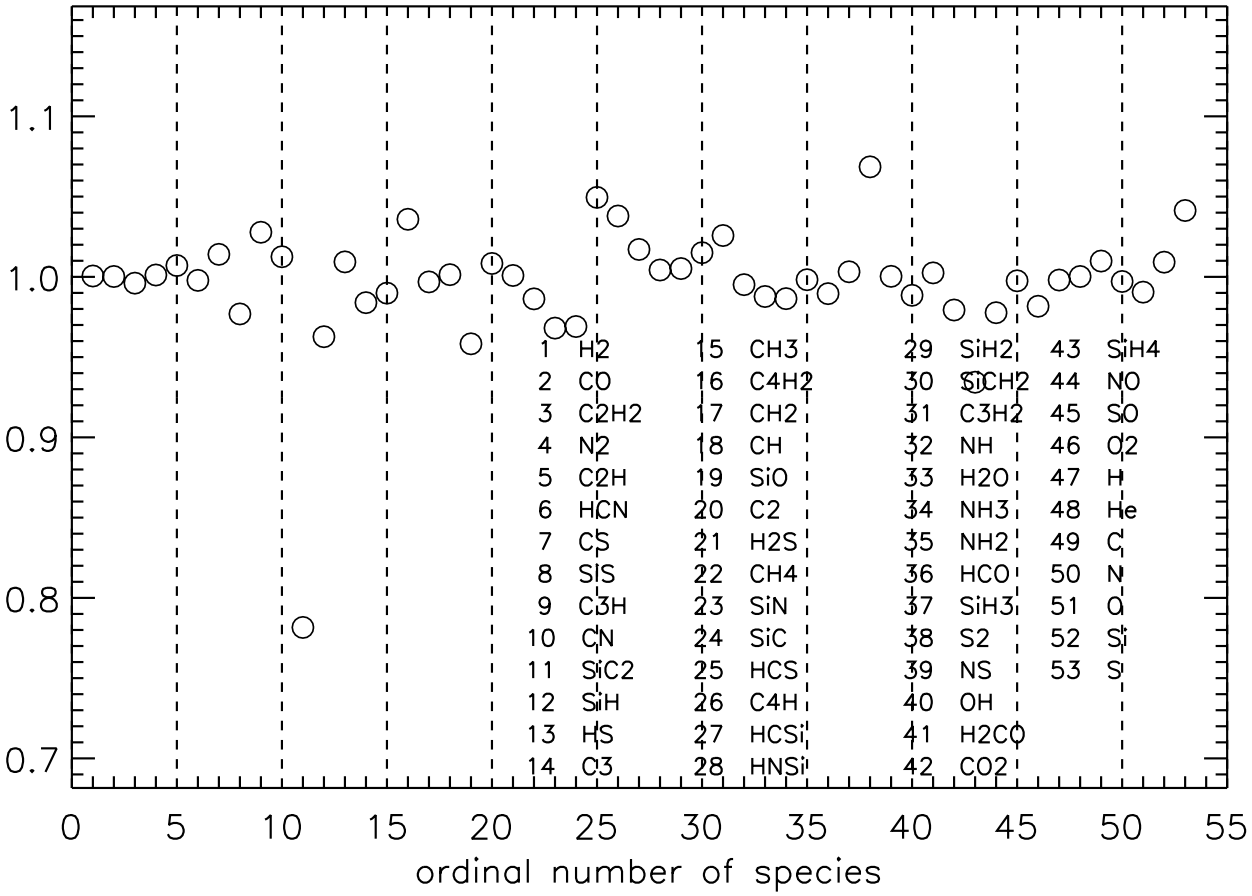


**Fig. 1.** The ratio of NIST and WC98 equilibrium concentrations. The order of species (except for elements on the right side of the figure) follows decreasing concentrations of WC98.

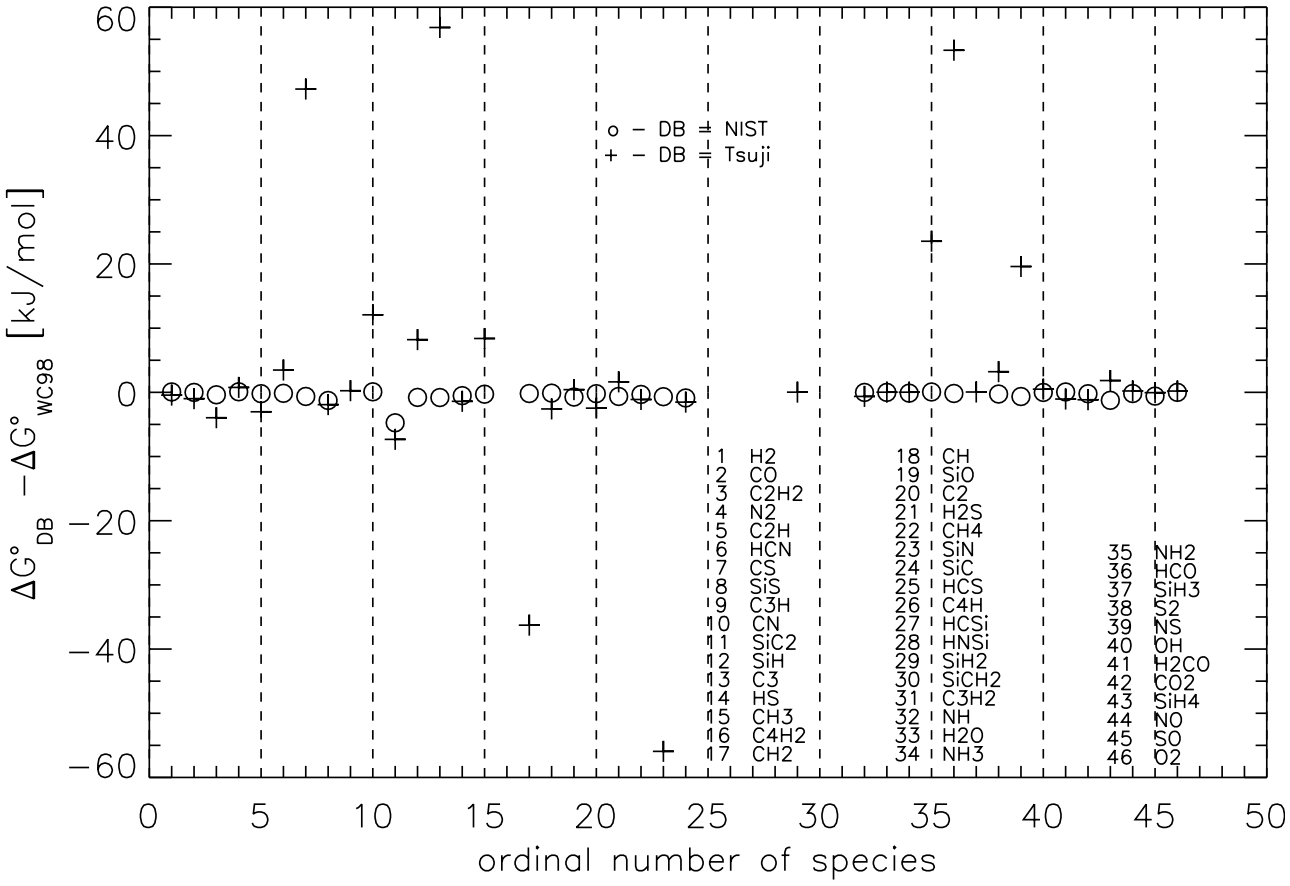


**Fig. 2.** The differences in $\Delta G^\circ$ between the database (DB: DB = NIST or Tsuji) and WC98. Results are marked by circles for the NIST database and by pluses for the Tsuji database. The order of species is same as in Fig. 1.

and NIST concentrations becomes much better (see red circles in Fig. 3[4]), especially for the family of all S-bearing molecules. A decrease in concentration of CS – #7 releases atomic carbon and sulfur, and the excess of sulfur increases concentrations of all S-bearing species. However at the same time, the increase in SiS – #8 concentration causes the decrease in concentration for all other silicon-bearing species, even for carbon-bearing ones: $SiC_2$ – #11 and SiC – #24. Therefore, it seems that the SiS molecule controls the silicon chemistry in this case. The considerable increase in concentration of sulfur monoxide (SO – #45) is caused by both an access to sulfur due to the decrease in $n_{CS}$ and an access to oxygen due to the decrease in $n_{SiO}$ (SiO – #19). Furthermore, the enrichment of the gas in carbon leads to increasing concentrations of all molecules composed of only C or carbon and hydrogen. Note that decreasing $\Delta G^\circ$ for NS – #39 (molecule with the second largest difference between $\Delta G^\circ$ in the NIST and Tsuji databases) would result in much better agreement between corresponding concentrations *only* for this molecule.

As a starting point for the second test we chose concentrations marked by the red circles in Fig. 3[4]. They are repeated now by black circles in Fig. 4[4]. The order of species is the same as in Fig. 1. Red circles in Fig. 4[4] now show the Tsuji concentrations relative to the NIST ones obtained after additional replacement of $\Delta G^\circ$ by the NIST values for all molecules, which show significant discrepancy in the Gibbs energies (i.e. for CN - #10, $SiC_2$ - #11, SiH - #12, $C_3$ - #13, $CH_3$ - #15, $CH_2$ - #17, SiN - #23, $NH_2$ - #35, HCO - #36, and NS - #39 – see Fig. 2 and Table 2). As we can see, changes in $\Delta G^\circ$ for these molecules almost alter only concentrations for these species. The exception is $C_3$, where the atomic carbon released by its decreasing abundance (due to the smaller $\Delta G^\circ$ in the NIST database) is also bound into other carbon-bearing molecules: $C_3H$ – #9, $SiC_2$ –#11, $C_4H_2$ – #16, $C_4H$ – #26, and $C_3H_2$ – #31.

Finally, we present results that show how relatively small changes of $\Delta G^\circ$ for abundant molecules like acetylene ($C_2H_2$ – #3) alter the equilibrium abundances of other molecules. The value of $\Delta G^\circ$ for acetylene from the Tsuji database is *only* about 3.6 [kJ/mol] lower than that from NIST (see Table 2). In Fig. 5[4] we present the ratio between the Tsuji and NIST equilibrium concentrations by black circles, while red circles show these ratios computed with $\Delta G^\circ$ replaced only for acetylene by the higher value from the NIST. As we can see, even this small change in $\Delta G^\circ$ for this parent and abundant molecule significantly alter the obtained concentrations for almost all other species. With higher $\Delta G^\circ$ for acetylene, more carbon is used for forming this molecule and therefore concentration of other C-bearing molecules are significantly decreased. This also affects concentrations of other species. In the case of silicon-bearing molecules, all silicon released from $SiC_2$ is bounded into SiS and SiO. The least sensitive to the change in $\Delta G^\circ$ for acetylene turned out to be such molecules as SiH – #12, HCS – #25, $SiH_2$ – #29, HCO – #36, $SiH_3$ – #37, $H_2CO$ – #41, and $SiH_4$ – #43.

## 3. Test of chemical codes: the chemical kinetics

In the outer part of the stellar atmospheres one can expect that non-TE effects are becoming greater and greater, so non-TE methods to determine properly concentrations of chemical species are necessary. We have developed a kinetic code to treat

time-dependent chemistry and describe the performed tests here. Now, however, instead of using dissociation constants (or equivalently $\Delta G^{\circ}$), we need to consider an appropriate reactions network. In this work we consider the reactions network of WC98.

### 3.1. The kinetic code and reaction network

To find molecular concentrations we have to consider all chemical reactions from the given network that lead to formation and destruction of all the molecules being studied. The evolution of concentration with time for species X can be written as

$$\frac{\mathrm{d}n_{\mathrm{X}}}{\mathrm{d}t} = F_{\mathrm{X}} - D_{\mathrm{X}}, \tag{9}$$

where the $F_{\mathrm{X}}$ stands for reactions responsible for production of species X, and $D_{\mathrm{X}}$ for its destruction.

The rate equations, defined for each considered reaction, are accumulated in the developed code. The rate equation describes the rate of disappearance of each of the reactants and, on the other hand, the appearance rate of each of the products. For example, for reaction $\mathrm{A} + \mathrm{B} \rightarrow \mathrm{C} + \mathrm{D}$, the rate equation is defined as

$$-\frac{\mathrm{d}n_{\mathrm{A}}}{\mathrm{d}t} = -\frac{\mathrm{d}n_{\mathrm{B}}}{\mathrm{d}t} = \frac{\mathrm{d}n_{\mathrm{C}}}{\mathrm{d}t} = \frac{\mathrm{d}n_{\mathrm{D}}}{\mathrm{d}t} = k\, n_{\mathrm{A}}^{\gamma}\, n_{\mathrm{B}}^{\delta}, \tag{10}$$

where $n_{\mathrm{A}}$, $n_{\mathrm{B}}$ are the concentrations of reactants, $n_{\mathrm{C}}$, $n_{\mathrm{D}}$ are the concentrations of products, and the parameters $\gamma$ and $\delta$ characterise the order of reaction with respect to each reactant. These parameters are derived experimentally, and their sum determines the reaction order. The coefficient $k$ in the above equation is known as a reaction rate constant, and it determines the reaction's dependence on the temperature. In our model the order of considered reactions was always the same as the reactants number; i.e. $\gamma$ and $\delta$ were equal 1.

We searched for the steady-state solution of the above set of rate equations using DVODE solver for systems of ordinary differential equation written at Lawrence Livermore National Laboratory[5]. DVODE solves the stiff system of differential equations of the first order, just like systems that are often met in the chemical kinetics. The solver must be updated with the subroutine providing the net reaction rates and eventually the subroutine providing Jacobian of the system. These two routines are constructed automatically by searching the network for given molecules and preparing a set of corresponding rate equations for a given range of temperature. The WC98 reaction network used in our study includes 53 species (7 elements and 46 molecules – given in Tables 1 and 2, respectively). The molecules are composed of six elements: H, C, N, O, Si, and S. Table 5 of WC98 gives data for 352 reactions. Among them there are 139 reactions in both directions (hereafter "two-way") and 213 reactions that do not have the backward reaction documented (hereafter "one-way", marked by "↔" in their table). However there are some misprints in this table:

1. The "two-way" reaction number 53 ($\mathrm{H_2} + \mathrm{N_2} \rightarrow \mathrm{NH} + \mathrm{NH}$) has a rate constant documented as zero. We computed this missing rate constant (by the method described below – see Eqs. (12) and (13)) using equilibrium constant and the rate constant for its backward reaction (i.e. for reaction number 269: $\mathrm{NH} + \mathrm{NH} \rightarrow \mathrm{H_2} + \mathrm{N_2}$). Note, however, that such an approach means that reaction 269 must be treated as a "one-way" process. After this change number of "one-way" reactions in network increased by one to 214, while the number of "two-way" reactions decreased to 137.
2. The reaction number 78 ($\mathrm{C} + \mathrm{NS} \rightarrow \mathrm{CS} + \mathrm{N}$) is indicated as a "two-way" reaction (there is no "↔" in the table), but this reaction does not have a documented backward reaction and, in fact, should be treated as a "one-way" process. This change means that number of "one-way" reactions increases to 215, while the number of "two-way" reactions decreases to 136.
3. The reaction number 217 ($\mathrm{S{+}N_2} \rightarrow \mathrm{S} + \mathrm{NS}$) is incorrect. It seems that the correct version of this reaction is $\mathrm{S{+}N_2} \rightarrow \mathrm{N} + \mathrm{NS}$. However, this reaction is already present in the network, therefore we simply deleted reaction number 217 from the list. This way, the number of "one-way" reactions decreases by one to 214.
4. The correct version of reaction 279 ($\mathrm{SiH} + \mathrm{NO} \rightarrow \mathrm{SiO} + \mathrm{H}$) should be $\mathrm{SiH} + \mathrm{NO} \rightarrow \mathrm{SiO} + \mathrm{NH}$. This does not change the statistics of reactions.

In summary, we have 564 reactions in the network according to Table 5 of WC98: 214 in "one-way" + 214 backward, determined as described below + 136 "two-way" reactions.

The rate constants for forward and backward reactions documented in Table 5 of WC98 were computed via equation in the Arrhenius form:

$$k_{\mathrm{f,b}} = A \left(\frac{T}{300}\right)^{\beta} \exp\left(-\frac{E_{\mathrm{a}}}{T}\right), \tag{11}$$

where $k_{\mathrm{f}}$ and $k_{\mathrm{b}}$ are the rate constants of forward and backward reactions, respectively, and $A$, $\beta$, and $E_{\mathrm{a}}$ are the Arrhenius parameters given in that table. In the case of missing backward reactions, WC98 calculated the backward rate constant $k_{\mathrm{b}}$ from the thermodynamics of the reaction (see Eq. (4) in WC98). In our computations the backward rate constant $k_{\mathrm{b}}$ for specific reaction and given temperature was derived from the ratio of rate constant for the forward reaction, and the reaction equilibrium constant $K_{\mathrm{r}}$, i.e.

$$k_{\mathrm{b}} = k_{\mathrm{f}}/K_{\mathrm{r}}. \tag{12}$$

On the other hand, the equilibrium constant for a given reaction can be obtained from the ratio of equilibrium concentrations for products and reactants. For example, for reaction $\mathrm{AB} + \mathrm{C} \rightarrow \mathrm{AC} + \mathrm{B}$, the corresponding equilibrium constant is given by

$$K_{\mathrm{r}} = \frac{n_{\mathrm{AC}} n_{\mathrm{B}}}{n_{\mathrm{AB}} n_{\mathrm{C}}}, \tag{13}$$

where $n_{\mathrm{AB}}$, $n_{\mathrm{C}}$, $n_{\mathrm{AC}}$, $n_{\mathrm{B}}$ are the equilibrium concentrations of reactants and products, respectively. Therefore after inserting $K_r$ given by Eq. (13) into Eq. (12) we have

$$k_{\mathrm{b}} = k_{\mathrm{f}} \frac{n_{\mathrm{AB}} n_{\mathrm{C}}}{n_{\mathrm{AC}} n_{\mathrm{B}}}. \tag{14}$$

Thus, by computing *missing* backward rate constants, we have modified the original network of WC98 to test our kinetic code.

### 3.2. Comparison of TE concentrations derived with WC98 and UDFA05 reaction networks

The chemical timescales in the dense and warm part of the envelope are very short, so the concentrations of species should reach the steady-state values very quickly. Therefore, to test our kinetic code we decided to reproduce the equilibrium concentrations of the 53 species discussed above. In a such case, we only need the initial concentrations of elements as an input to the code (values are taken from Table 1), the total gas density and its temperature

[5] http:://www.llnl.gov/CASC/odepack/

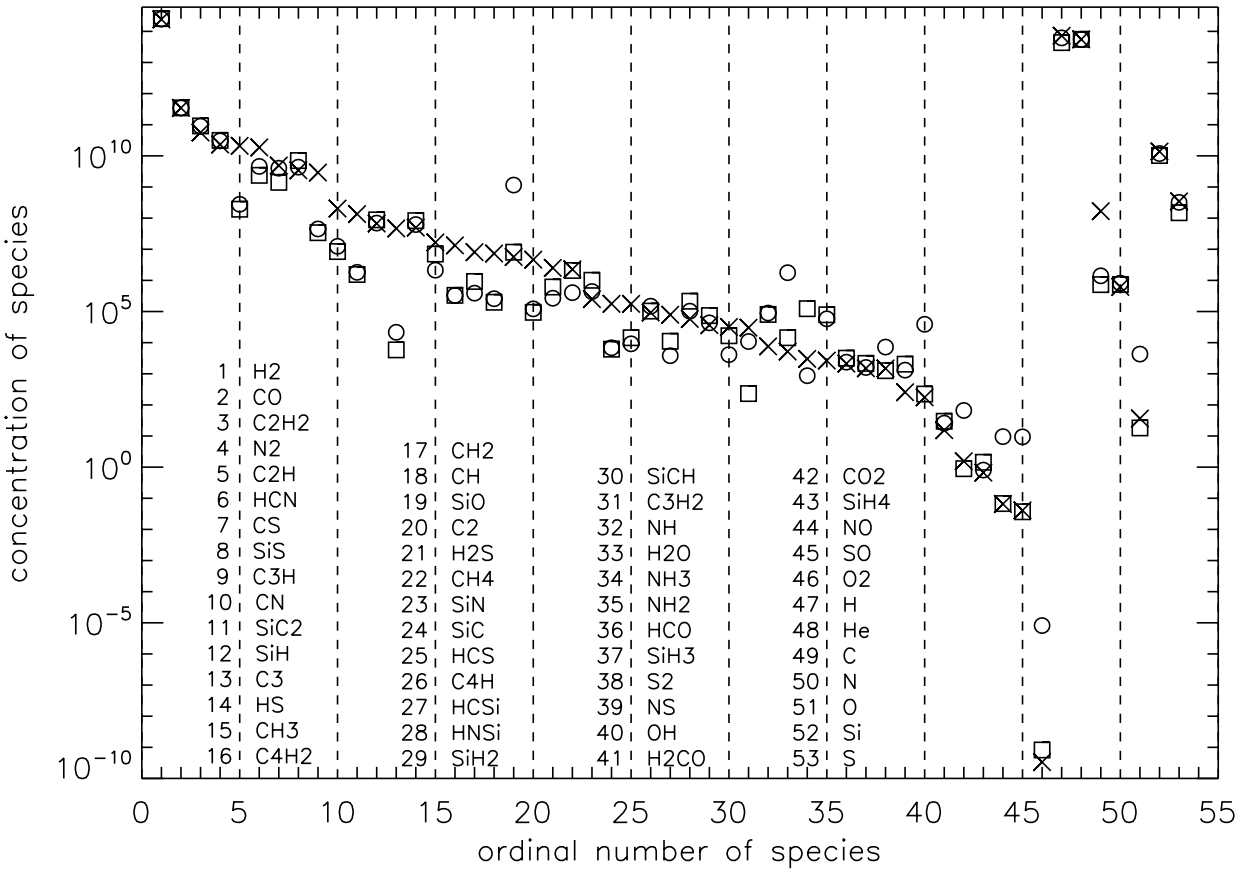


**Fig. 6.** Comparison between species concentrations in [$cm^{-3}$] derived by our kinetic code for case 1 – crosses, and for case 2 – circles, at conditions specified in the 1st entry of Table 2 in WC98. Squares mark the concentration for case 2, with rate constants updated using the UDFA05 database. The order of species is the same as in Fig. 1.

(again we adopted physical conditions specified in the 1st entry of Table 2 in WC98).

To test our chemical kinetic code, we adopted rate constants only for the forward reactions[6] (282 = 136/2+214 – the network of WC98 requires the rate equations for 564 reactions) and computed the rate constants for all (282) backward reactions according to the method described above (hereafter case 1). As expected, in this case our code reproduces the WC98 equilibrium concentrations (crosses in Fig. 6). The species (except for atoms collected on the right side of the plot) are plotted in order of decreasing abundances. In addition, we tested the stability of our code by assuming that the initial chemical composition of all species is equal to that at the thermodynamical equilibrium for these conditions. No changes in the species concentrations were seen after a very long time ($10^8$ s). Therefore, for further computations we used the equilibrium concentrations as an input to our code (for its faster convergence). Note that the results are the same when we start with purely atomic gas.

In the next test (hereafter case 2) we took all rate constants available in the WC98 network (i.e. 350 = 214 + 136 – see the previous subsection) and computed the rate constants only for the missing (214) backward reactions by using NIST thermochemical data (in fact, this approach is the same as described by WC98). The results are presented in Fig. 6 as circles. It is seen that the present steady state differs from the thermodynamical equilibrium concentrations (case 1). More detailed comparison for all species that belong to a given family (molecules containing element: H, C, N, O, Si, and S, respectively) are presented in six panels in Fig. 7[4] as circles going from the left to right and from the top to bottom for: H, C, N, O, Si, and S. For each panel we defined the separate ordinal number of species according to decreasing equilibrium concentrations with the exception of atom(s) shown on the right side of each panel.

The inconsistency in species abundances is rather high and only fifteen species differ less than 30% (i.e. He, CO, $H_2$, SiH, $SiH_3$, S, HCO, Si, H, CS, $SiH_2$, $SiH_4$, HS, SiS, $N_2$, and N). The greatest differences are seen for oxygen-based molecules. Only formyl (HCO) and the most abundant among O-bearing molecules – carbon monoxide (CO) – are in relatively good agreement with the corresponding equilibrium concentrations. Concentrations of other molecules (i.e. SiO, $H_2O$, OH, $H_2CO$, $CO_2$, NO, SO, and $O_2$) are far from equilibrium values.

The WC98 network was created on the basis of the RATE95 database (Millar et al. 1997). The discrepancies present in the above results encourage us to update the rate constants using the UDFA05 database (Woodall et al. 2007). We found that 162 reactions among 564 now have the new values of the rate constants. We performed the same test as in case 2 (i.e. only missing backward rates were computed using Eq. (14)) with the reaction network updated using the UDFA05 database. The results are presented as squares in Fig. 6, and the family splitting in this case is also shown in Fig. 7[4] by squares.

[6] As a forward reaction, among reactions with rate constants given for both directions, we chose the reaction with more precise rate constant i.e. first when Arrhenius parameter $\beta$ (see Eq. (11)) is different from zero. If $\beta = 0$ for both reactions, we took the reaction with the smaller Arrhenius parameter $E_a$. In the case of reactions without the backward rate constants, we treat all of them as a forward reactions.

The agreement with the equilibrium state for oxygen-bearing molecules is now much better. However, the discrepancies in abundances of carbon-bearing molecules are still present. Moreover, the differences with equilibrium results for nitrogen-bearing molecules are even higher.

The most likely source of inconsistency is the problem with determining reaction rate constants for the silicon- and sulfur-bearing species. WC98 estimated the rate constants for these reactions from similar reactions involving covalent species, i.e. oxygen for sulfur and carbon for silicon (see comments in Table 5 of WC98). When this group of reactions was excluded from the studied network, the abundances of carbon-bearing and oxygen-bearing molecules became more consistent with LTE results. However, the results for nitrogen-bearing species are still unsatisfactory, so additional work on the chemical network extension is needed.

## 4. Conclusions

In this paper we have tested our chemical (equilibrium and kinetic) codes to use them during self-consistent modelling of dynamics and chemistry in outflows from C-rich AGB stars.

The LTE molecular distribution at the base of the wind is needed as the boundary condition for determining the chemical composition in the circumstellar envelope of the AGB star. In such LTE calculations it is necessary to keep in mind the possible influence of the different sets of equilibrium dissociation constants on the species concentration. Analysis of the conducted test calculations shows that, fortunately, this influence on less abundant molecules is rather weak. However, for more abundant species, the influence is crucial and the chosen sets of equilibrium dissociation constants should be carefully selected and checked. In particular, our calculations have shown that the NIST database reproduces the WC98 equilibrium concentrations well, while agreement between WC98 and Tsuji is much less.

The steady-state solution obtained with the kinetic code for the WC98 reactions network is different from the thermodynamical equilibrium solution. This would affect the full time-dependent radiative-hydrodynamic computations of the inner wind. Note that CN and $C_2$ molecules, important for the opacity computations in the atmosphere of a carbon-rich star, are underabundant by more than one order of magnitude in comparison to equilibrium concentration (see Fig. 6). Our kinetic computations also show the strong overabundance of oxygen-bearing molecules (especially of SiO, $H_2O$, and OH) in comparison to the LTE approach. It would be interesting to investigate how these overabundances influence the final results of the inner wind studies by Willacy & Cherchneff (1998) and Cherchneff (2006).

To make both the LTE and kinetic models consistent, we propose to replace all reaction rates in a backward direction[7] by reaction rates computed from forward reactions by using thermochemical data. Then, in the limit of high density and temperature (i.e. when chemical timescales are much shorter than dynamical timescales), the kinetic steady-state solution approached the local thermodynamical equilibrium.

Observations (Tsuji et al. 1973) and the astrochemical modelling (WC98, Cherchneff 2006) both show that the base of inner wind in AGBs is a region of active chemistry. Therefore, the chemical network, which may be used to investigate the composition of this region, should include an extended set of chemical reactions, such as neutral-neutral, involving metals and photochemistry induced by the stellar radiation field. This will be direction of our future studies.

*Acknowledgements.* We are very indebted to the referee, Karen Willacy, for providing us with the original Gibbs free energies used in WC98 and for comments that allowed us to improve the manuscript.

This work has been partly supported by grants 2.P03D 017.25 and 1.P03D.010.29 of the Polish State Committee for Scientific Research.

## References

Asplund, M., Grevesse, N., & Sauval, A. J. 2005, ASPC, 336, 25 (A05)
Cherchneff, I. 2006, A&A, 456, 1001
Glassgold, A. E. 1996, ARA&A, 34, 241
Grevesse, N., & Sauval, A. J. 1998, SSRv, 85, 161 (GS98)
Millar, T. J. 2003, Molecule and Grain Formation in Asymptotic Giant Branch Stars, ed. H. J. Habing, & H. Olofsson (NY: Springer), 247
Millar, T. J., Farquhar, P. R. A., & Willacy, K. 1997, A&AS, 121, 139
Olofsson, H. 2006, Rev. Mod. Astron., 19, 75
Pulecka, M., Schmidt, M., Shematovich, V., & Szczerba, R. 2005a, dmu. Conf, 457
Pulecka, M., Schmidt, M., Shematovich, V., & Szczerba, R. 2005b, IAUS, 231, 71
Russell, H. N. 1934, ApJ, 79, 317
Tsuji, T. 1973, A&A, 23, 411
Tsuji, T., Ohnaka, K., Aoki, W., & Yamamura, I. 1973, A&A, 320, L1
Willacy, K., & Cherchneff, I. 1998, A&A, 330, 676 (WC98)
Woodall, J., Agundez, M., Markwick-Kemper, A. J., & Millar, T. J. 2007, A&A, 466, 1197

[7] See footnote 6.

# Online Material

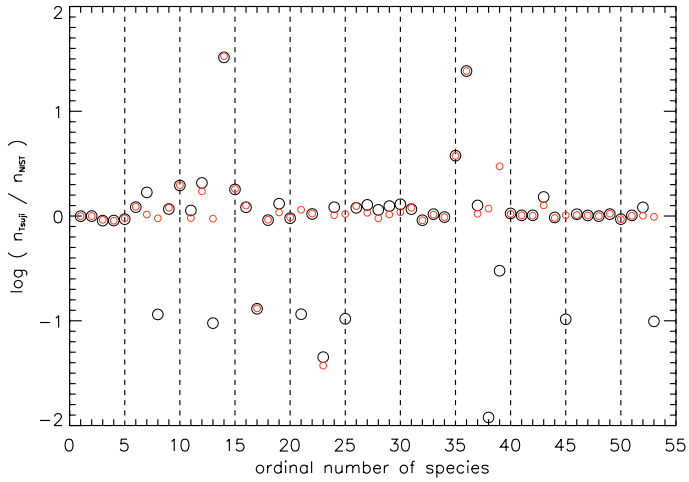


**Fig. 3.** The ratio between Tsuji and NIST equilibrium concentrations at conditions specified in Sect. 2.2 – black circles. Red circles mark the ratio, when $\Delta G^\circ$ for CS in the Tsuji database was replaced by the value from WC98. The order of species is same as in Fig. 1.

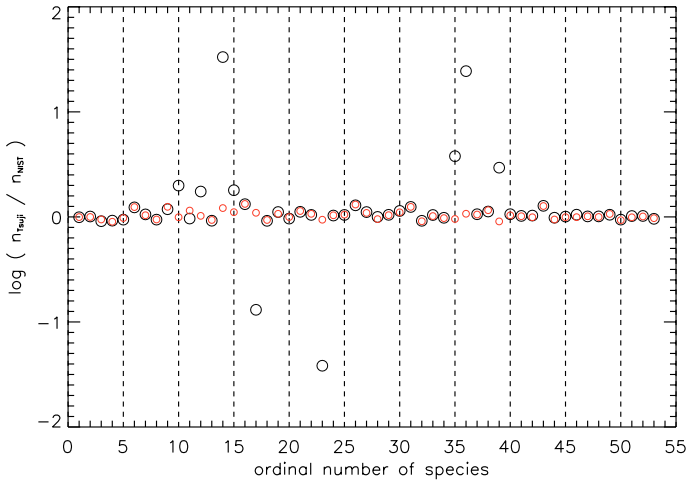


**Fig. 4.** The ratio between Tsuji (with $\Delta G^\circ$ for CS replaced by the value from NIST) and NIST equilibrium concentrations at conditions specified in Sect. 2.2 – black circles. Red circles mark the ratio, with additional replacement of $\Delta G^\circ$ for CS, CN, $SiC_2$, SiH, $C_3$, $CH_3$, $CH_2$, SiN, $NH_2$, HCO, and NS in the Tsuji database by the values from WC98. The order of species is same as in Fig. 1.

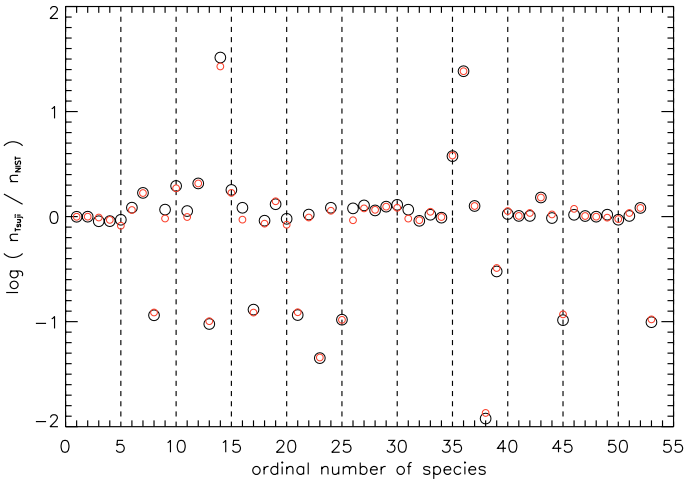


**Fig. 5.** The ratio between Tsuji and NIST equilibrium concentrations at conditions specified in Sect. 2.2 – black circles. Red circles mark the ratio, when $\Delta G^\circ$ for $C_2H_2$ in the Tsuji database was replaced by the value from NIST. The order of species is same as in Fig. 1.

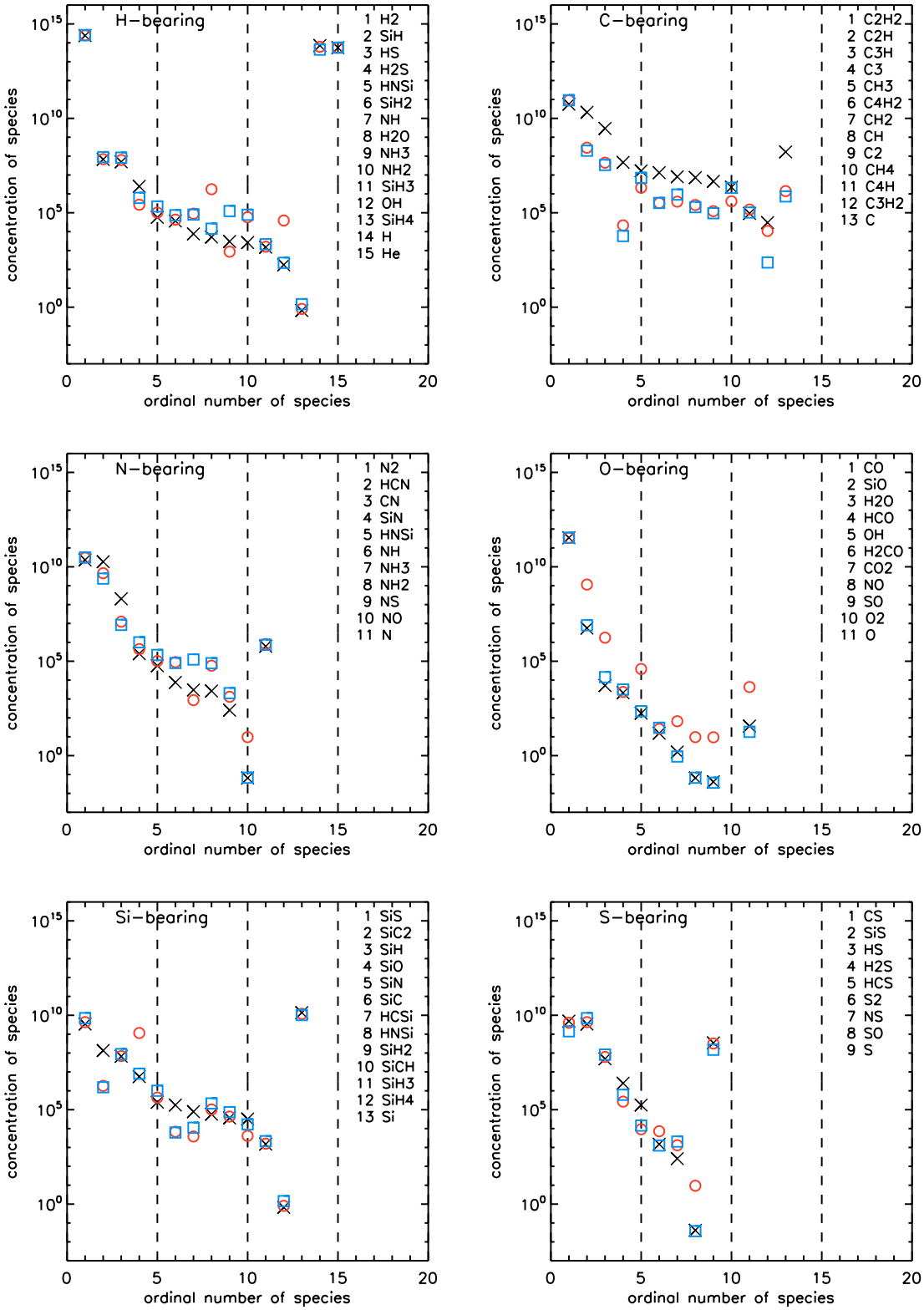


**Fig. 7.** The network balance. Comparison of species concentrations in [$cm^{-3}$] computed for the modified WC98 network (case 1 – crosses), which are consistent with the TE solution, and for the WC98 network (case 2 – circles). Squares mark a case similar to case 2, with rate constants updated using data from the UDFA05 database. The concentrations are split into H-bearing, C-bearing, N-bearing, O-bearing, Si-bearing, and S-bearing molecules. For each panel we defined the separate ordinal number of species according to decreasing equilibrium concentrations with the exception of atom(s), which are shown on the right side of each panel.